
[View Journal Online](#)
[View Article Online](#)

Synthesis, spectroscopic characterization, crystal structure and computational studies of two new *N*-aroyl-*N'*-(2,4,6-tribromophenyl)thioureas

 Nahide Burcu Arslan ¹ and Fatma Aydin ^{2,*}
¹ Department of Computer Education and Instructional Technology, Faculty of Education, Giresun University, 28200, Giresun, Turkey

² Department of Chemistry, Faculty of Science, Canakkale Onsekiz Mart University, 17100, Canakkale, Turkey

 * Corresponding author at: Department of Chemistry, Faculty of Science, Canakkale Onsekiz Mart University, 17100, Canakkale, Turkey.
 e-mail: faydin@comu.edu.tr (F. Aydin).

RESEARCH ARTICLE



doi: 10.5155/eurjchem.15.2.155-165.2551

Received: 15 March 2024

Received in revised form: 16 April 2024

Accepted: 4 May 2024

Published online: 30 June 2024

Printed: 30 June 2024

KEYWORDS

 Single crystal structure
 HOMO and LUMO analysis
 X-ray structure determination
 Electronic structure properties
 Molecular electrostatic potential
N-Benzoyl-*N'*-tribromophenylthiourea

ABSTRACT

Two new compounds, *N*-benzoyl-*N'*-tribromophenylthiourea (I) and 4-nitrobenzoyl-*N'*-tribromophenylthiourea (II), were synthesized and characterized by ¹H NMR, ¹³C NMR, IR, and X-ray single crystal diffraction techniques. The molecular geometry of compounds I and II in the ground state has been calculated by using the density functional theory (DFT) method with the B3LYP/6-311G(d,p) basis set and compared with the experimental data. The calculated results show that the optimized geometry can reproduce well the crystal structural parameters. A detailed vibrational spectral analysis has been carried out, and assignments of the observed fundamental bands have been proposed on the basis of peak positions. The scaled theoretical frequencies show very good agreement with the experimental values. Frontier molecular orbitals energies (HOMO and LUMO), energy gap, and global chemical reactivity parameters such as ionization potential, electron affinity, chemical hardness, and chemical softness have been calculated, and the sites of electrophilic and nucleophilic regions where the molecular interactions likely to happen are identified. The molecular electrostatic potential and thermodynamic properties of the title compounds were investigated by theoretical calculations.

 Cite this: *Eur. J. Chem.* 2024, 15(2), 155-165

 Journal website: www.eurjchem.com

1. Introduction

The derivatives of aroyl/acylthiourea due to the heteroatom content are known for their several biological activities, including antifungal, antibacterial, antiviral, insecticidal, herbicidal, *etc.* effects [1-5]. They are an important class of organic compounds having O-, N- and S-atoms. The amide, carbonyl, thioamide, and thiocarbonyl groups of the C(O)-NH-C(S)-N core fragment that can participate in the tautomer are in the same molecule [6,7] leading to physicochemical and biological properties suitable for application in the field of coordination chemistry [8-10]. In addition, their derivatives consist of heteroatoms such as nitrogen and sulfur, which are nucleophilic centers, allowing the formation of intermolecular and intramolecular hydrogen bonds in the crystal structure [11-13]. Steric hindrance slows down chemical reactions due to steric mass [14]. Generally, steric hindrance gains importance in intermolecular reactions, but it also determines intermolecular interactions in the crystal lattice structure [15]. In addition, it is often used to control selectivity, such as slowing down undesired side reactions [16,17].

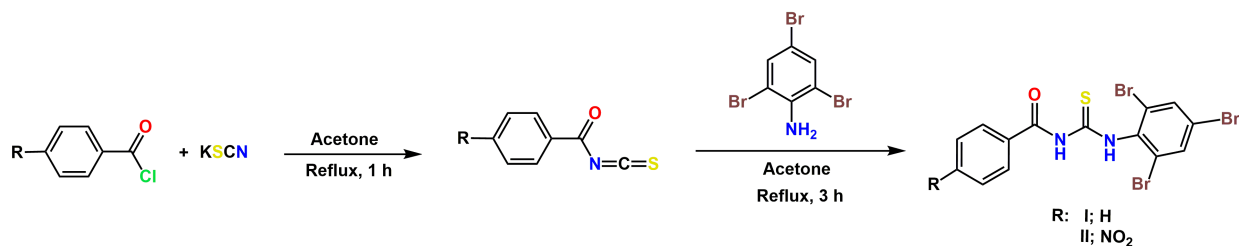
In the present work, two novel compounds, *N*-benzoyl-*N'*-(2,4,6-tribromophenyl)thiourea (I) and *N*-4-nitrobenzoyl-*N'*-(2,4,6-tribromophenyl) thiourea (II) were synthesized in high

yield, via aroyl isocyanates and 2,4,6-tribromoaniline (Scheme 1). The structural characterization of compounds I and II has been confirmed using FT-IR and NMR spectroscopy techniques and a single crystal X-ray diffraction method. The unit cells of the crystal were compared with similar molecules in terms of steric hindrance. The geometrical parameters of the title compounds in the ground state have been calculated using the density functional theory (DFT) method with the B3LYP/6-311G (d,p) basis set and the experimental data were compared. After optimization of molecular geometry, the molecular electrostatic potential (MEP) map, the highest occupied molecular orbital (HOMO) and the lowest unoccupied molecular orbital (LUMO) analyzes, and thermodynamic properties were calculated by using density functional theory (DFT) at the B3LYP/6-311G(d,p) level.

2. Experimental

2.1. Material and measurements

All reagents (except 2,4,6-tribromoaniline) and solvents used in the synthesis were commercially purchased from Sigma-Aldrich, Merck Chemical.



Scheme 1. Synthesis pathway of compounds I and II.

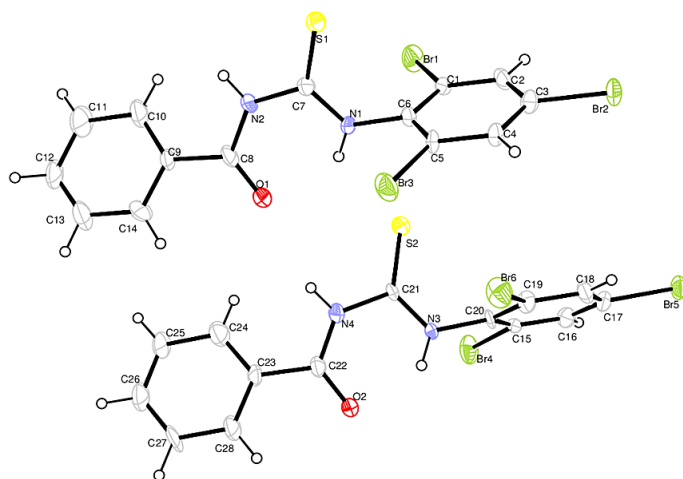


Figure 1. A view of compound I with the atom-numbering scheme. Displacement ellipsoids are drawn at the 30% probability level, and H atoms are shown as small spheres of arbitrary radii.

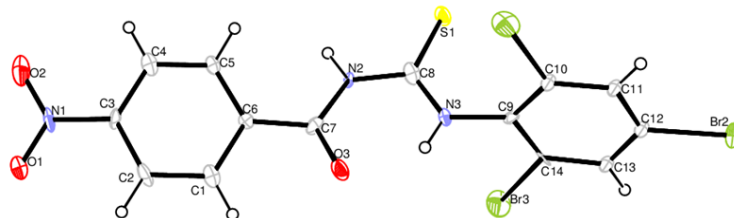


Figure 2. A view of compound II, showing the atom-numbering scheme. Displacement ellipsoids are drawn at the 30% probability level, and H atoms are shown as small spheres of arbitrary radii.

The melting points were determined in open capillary tubes using an IA 9100 Electrothermal apparatus. Reactions were monitored by thin layer chromatography (TLC) on silica gel 60F₂₅₄ plates (Merck). The infrared (FT-IR) spectrums were recorded on the PerkinElmer Spectrum 100 FT-IR spectrometer in a spectral range of 4000–650 cm⁻¹. The ¹H NMR and ¹³C NMR spectra were recorded on a JEOL ECX-400 FT-NMR spectrometer operating at 400 and 100 MHz, respectively, using DMSO-*d*₆ as a solvent. Crystal structure analyzes of the title compounds were carried out using a Bruker APEX-II CCD X-ray diffractometer (MoK α radiation, λ = 0.71073 Å).

2.2. Synthesis and characterization

2,4,6-Tribromoaniline was synthesized in the literature [15]. A solution of aryl chloride (benzoyl- and 4-nitrobenzoyl, 2.32 mL and 3.70 g, 20 mmol, respectively) in dry acetone (20 mL) was added dropwise to a round bottom three-neck flask containing potassium thiocyanate solution in acetone (10 mL) (1.94 g, 20 mmol). The mixtures were refluxed for approximately 1 hour and then cooled to room temperature. Then, a solution of 2,4,6-tribromoaniline (0.652 g, 20 mmol) in dry

acetone (20 mL) was added dropwise over 0.5 h, without filtration obtained white benzoyl isothiocyanate and pale yellow 4-nitrobenzoyl isothiocyanate, and the mixture was stirred for 2 and 3 h, respectively. The resulting mixture was pushed into 100 mL of water and filtered, washed with hot water to remove inorganic salts, and dried under vacuum. Subsequently, the raw product was chromatographed on silica gel using ethyl acetate: hexane (4:1, *v:v*) as an eluent to separate the product. After evaporation of the solvent, the fairly pure, colorless (I) and pale-yellow (II) products were crystallized, respectively (Scheme 1).

N-Benzoyl-*N'*-(2,4,6-tribromophenyl)thiourea (I): Color: Colorless. Yield: 0.857 g, 87%. M.p.: 207–208 °C. ¹H NMR (400 MHz, DMSO-*d*₆, δ , ppm): 12.08 (s, 1H, NH), 11.94 (s, 1H, NH), 8.04 (s, 2H, Ar(Br)₃-H), 8.02 (d, *J* = 7.7 Hz, 2H, Ar-H), 7.69 (t, 2H, Ar-H), 7.56 (s, 1H, Ar-H). ¹³C NMR (100 MHz, DMSO-*d*₆, δ , ppm): 180.75 (C=S), 168.04 (C=O), 136.94, 131.71, 128.50, 121.40 (Ar(Br)₃-C), 134.23, 133.34, 128.76, 125.08 (Ph-C). FT-IR (ATR, *v*, cm⁻¹): 3255 (N-H), 3112 (N-H), 3099, 3074, 3003 (C_{ar}-H), 1670 (C=O), 1603 (C=C), 1506 (N-CS, thioureido), 1343 (N-CO), 1262 cm⁻¹ (CS-N), 861 (C=S, stretching), 778, 739, 701 (C-Br).

Table 1. Crystal data and structure refinement parameters for compounds I and II.

Parameters	Compound I	Compound II
Empirical formula	C ₁₄ H ₆ Br ₃ N ₂ O ₃ S	C ₁₄ H ₈ Br ₃ N ₃ O ₃ S
Formula weight	493.02	538.02
Temperature (K)	293	293
Crystal system	Monoclinic	Orthorhombic
Space group	<i>P2₁/n</i>	<i>Pbca</i>
a, (Å)	8.0437(13)	16.5477(12)
b, (Å)	37.021(6)	7.4257(6)
c, (Å)	10.7842(15)	28.378(2)
Volume (Å ³)	3210.9(8)	3487.1(5)
Z	8	8
ρ _{calc} (g/cm ³)	2.040	2.050
α, β, γ (°)	90, 90.936 (5), 90	90, 90, 90
μ (mm ⁻¹)	7.666	7.077
F(000)	528.0	528.0
Crystal size (mm ³)	0.12×0.09×0.07	0.09×0.07×0.03
Colour / Shape	Colourless / Prism	Pale yellow / Block
Radiation	MoKα (λ = 0.71073)	MoKα (λ = 0.71073)
2θ range for data collection (°)	2.9 ≤ θ ≤ 26	2.9 ≤ θ ≤ 25.1
Reflections collected	36579	27641
Independent reflections	6301	3061
Data/restraints/parameters	6301/0/380	3061/0/181

N-4-Nitro-benzoyl-*N'*-(2,4,6-tribromophenyl)thiourea (II): Color: Pale yellow. Yield: 0.775 g, 72 %. M.p.: 221-222 °C. ¹H NMR (400 MHz, DMSO-*d*₆, δ, ppm): 12.25 (s, 1H, NH), 11.86 (s, 1H, NH), 8.31 (d, 2H, Ar(NO₂)-H), 8.17 (d, *J* = 7.7 Hz, 2H, Ar(NO₂)-H), 7.99 (s, 2H, Ar(Br)₃-H). ¹³C NMR (100 MHz, DMSO-*d*₆, δ, ppm): 180.91 (C=S), 167.09 (C=O), 138.04, 134.78, 125.56, 122.04 (Ar(Br)₃-C), 150.46, 137.42, 130.91, 123.95 (Ar(NO₂)-C). FT-IR (ATR, ν, cm⁻¹): 3413 (N-H), 3284 (N-H), 3180, 3095, 3073 (C_{aromatic}-H), 1728 (C=O), 1607 (C=C), 1539 (N-CS, thioureido), 1381 (-N-CO), 1276 (CS-N), 1346 (ON=O), 858 (C=S stretching) and 729, 705, 700 (C-Br).

2.3. X-ray data collection and structure refinement

The single-crystal X-ray data were collected on a Bruker APEX-II. All diffraction measurements were performed at room temperature (296 K) using graphite monochromated MoKα radiation (λ = 0.71073 Å). Unit cell parameters were determined from the least-squares refinement of setting angles with θ for compounds I and II in the range of 2.9 ≤ θ ≤ 26 and 2.9 ≤ θ ≤ 25.1, respectively. The structures were solved by direct methods using SHELXS-97 [18] implemented in the WinGX [19] program suite. The refinement was carried out using the full-matrix least squares method on the positional and anisotropic temperature parameters of the nonhydrogen atoms, or equivalently corresponding to 380 crystallographic parameters for compound I and 181 crystallographic parameters for compound II, using SHELXL-97 [18]. All H atoms of compound I and compound II were geometrically positioned and treated using a riding model, fixing the bond lengths at 0.86 and 0.93 Å for the NH and CH atoms, respectively. Details of the data collection conditions and refinement process parameters for the two compounds are given in Table 1. Bond lengths and angles for compounds I and II are given in Tables 2 and 3, respectively. Atomic numbering schemes with displacement ellipsoids of crystal structures drawn with ORTEP III [19] were depicted at the 30% probability level for clarity (Figures 1 and 2).

2.4. Computational procedures

The ground-state geometry of title compounds I and II that are taken from the crystal structure was optimized using the standard density functional theory (DFT) [20] level of B3LYP [21] with a basis set 6-311G(d,p) [22] using the Gaussian 09 program [23]. After optimization, quantum chemical calculations were made and a MEP surface map [24] was obtained. Thus, from the results of the MEP map, the chemical reactivity

of the compound could be easily estimated. Additionally, the HOMO-LUMO gaps and the FT-IR spectrum were calculated on the same basis set. The calculated vibrational frequencies of the optimized molecular structure were then scaled by 0.962 [25] for DFT. The vibrational band assignments were performed using the Gauss-View molecular visualization program [26].

3. Results and discussion

3.1. Description of the crystal structure

As shown in Figures 1 and 2, the crystals of compounds I and II crystallize in the monoclinic space group *P2₁/n* and the orthorhombic space group *Pbca*, respectively, with *Z* = 8. Both molecules have thiourea, 2,4,6-tribromophenyl and phenyl groups in common. The torsion angles between the 2,4,6-tribromophenyl and thiourea groups in the title compounds are 96.2 and 84.0°, respectively. In compound I, the molecular packing contains three different types of hydrogen bonds between C-H...Br, N-H...O, and N-H...S atoms, which are tabulated in Table 4. The N atom of the thiourea group acts as a donor atom to the benzoyl oxygen atom with the donor acceptor distance 3.273 Å and symmetry code (*x*, *y*, *z*-1). The other N atom of the same thiourea group also acts as a donor to the thiourea group S atom with the donor acceptor distance 3.353 Å and the symmetry code (*x*, *y*, *z*+1). The combination of these hydrogen bonds generates an R₂²(10) ring running parallel to [001], Figure 3. Similarly to compound I, compound II has a N-H...S type hydrogen bonding with donor acceptor distance 3.616 Å and symmetry code (-*x*+1, -*y*+2, -*z*+1). This bonding generates the R₁¹(8) ring running parallel to [100]. Furthermore, there is an intramolecular hydrogen bond between the thiourea N atom and the benzoyl O atom, as seen in Table 4 and Figure 4.

3.2. Spectral analysis

3.2.1. Vibrational spectra

The analysis of the experimental spectra of compounds I and II was supported by theoretical calculations using the B3LYP/6-311G(d,p) level of approximation (Figures 5 and 6). In addition, some vibration modes expected for compounds I and II of the title are presented in Table 5. The N-H stretching vibrations generally appear in 3300-3500 cm⁻¹ [27,28]. In the IR spectrum, the stretching vibrations of the amide group observed at 3255 and 3413 cm⁻¹ are assigned to the NH stretching mode of compounds I and II, respectively [29].

Table 2. Bond lengths and angles for compound I.

Atom	Atom	Length (Å)	Atom	Atom	Length (Å)		
C1	C2	1.392(18)	C15	C16	1.309(19)		
C1	C6	1.409(19)	C15	C20	1.42(2)		
C1	Br1	1.859(13)	C15	Br4	1.889(15)		
C2	C3	1.37(2)	C16	C17	1.38(2)		
C3	C4	1.423(19)	C17	C18	1.36(2)		
C3	Br2	1.887(14)	C17	Br5	1.882(14)		
C4	C5	1.418(17)	C18	C19	1.416(18)		
C5	C6	1.34(2)	C19	C20	1.38(2)		
C5	Br3	1.854(14)	C19	Br6	1.900(14)		
C6	N1	1.421(17)	C20	N3	1.448(16)		
C7	N1	1.336(19)	C21	N3	1.309(18)		
C7	N2	1.414(17)	C21	N4	1.430(16)		
C7	S1	1.643(16)	C21	S2	1.643(15)		
C8	C9	1.478(19)	C22	C23	1.505(19)		
C8	N2	1.367(19)	C22	N4	1.341(19)		
C8	O1	1.219(18)	C22	O2	1.222(18)		
C9	C10	1.41(2)	C23	C24	1.40(2)		
C9	C14	1.35(2)	C23	C28	1.36(2)		
C10	C11	1.42(2)	C24	C25	1.40(2)		
C11	C12	1.42(3)	C25	C26	1.37(3)		
C12	C13	1.22(3)	C26	C27	1.32(3)		
C13	C14	1.42(3)	C27	C28	1.39(2)		
Atom	Atom	Atom	Angle (°)	Atom	Atom	Atom	Angle (°)
C2	C1	C6	119.4(13)	C20	C15	Br4	117.6(10)
C2	C1	Br1	118.3(11)	C15	C16	C17	121.7(15)
C6	C1	Br1	122.2(10)	C16	C17	Br5	120.6(12)
C3	C2	C1	119.7(13)	C18	C17	C16	119.9(13)
C2	C3	C4	121.2(13)	C18	C17	Br5	119.5(11)
C2	C3	Br2	121.0(11)	C17	C18	C19	118.7(14)
C4	C3	Br2	117.8(10)	C18	C19	Br6	117.9(11)
C5	C4	C3	117.8(12)	C20	C19	C18	121.3(14)
C4	C5	Br3	116.8(10)	C20	C19	Br6	120.8(10)
C6	C5	C4	120.4(13)	C15	C20	N3	123.5(13)
C6	C5	Br3	122.8(10)	C19	C20	C15	116.5(12)
C1	C6	N1	119.1(13)	C19	C20	N3	119.9(14)
C5	C6	C1	121.5(12)	N3	C21	N4	113.1(12)
C5	C6	N1	119.3(13)	N3	C21	S2	127.8(10)
N1	C7	N2	115.0(13)	N4	C21	S2	119.0(11)
N1	C7	S1	125.2(11)	N4	C22	C23	116.8(14)
N2	C7	S1	119.8(12)	O2	C22	C23	120.5(14)
N2	C8	C9	115.7(15)	O2	C22	N4	122.7(13)
O1	C8	C9	122.6(14)	C24	C23	C22	121.7(14)
O1	C8	N2	121.6(13)	C28	C23	C22	119.5(15)
C10	C9	C8	121.4(14)	C28	C23	C24	118.2(14)
C14	C9	C8	118.5(16)	C25	C24	C23	118.7(18)
C14	C9	C10	119.5(15)	C26	C25	C24	119.5(19)
C9	C10	C11	117.8(18)	C27	C26	C25	121.9(17)
C10	C11	C12	118(2)	C26	C27	C28	119.5(19)
C13	C12	C11	122(2)	C23	C28	C27	121.7(19)
C12	C13	C14	122(2)	C7	N1	C6	123.0(12)
C9	C14	C13	120(2)	C8	N2	C7	129.5(13)
C16	C15	C20	122.0(14)	C21	N3	C20	122.2(12)
C16	C15	Br4	120.3(13)	C22	N4	C21	129.4(13)

Table 3. Bond lengths and angles for compound II.

Atom	Atom	Length (Å)	Atom	Atom	Length (Å)		
C6	C1	1.40(3)	C2	C3	1.36(3)		
C6	C5	1.40(3)	C3	C4	1.38(3)		
C6	C7	1.46(3)	C3	N1	1.41(3)		
C13	C14	1.38(3)	C5	C4	1.35(3)		
C13	C12	1.38(3)	C7	N2	1.38(2)		
C8	N3	1.33(3)	C7	O3 ¹	1.22(2)		
C8	N2	1.37(3)	C7	O3	1.22(2)		
C8	S1	1.66(2)	C10	C9	1.39(3)		
C11	C12	1.37(3)	C10	Br1	1.89(2)		
C11	C10	1.38(3)	C9	N3	1.41(2)		
C14	C9	1.38(3)	N1	O2	1.22(3)		
C14	Br3	1.90(2)	N1	O1	1.19(2)		
C12	Br2	1.91(2)	O3	O3 ¹	0.00(5)		
C2	C1	1.40(3)					
Atom	Atom	Atom	Angle (°)	Atom	Atom	Atom	Angle (°)
C1	C6	C5	117.9(19)	C5	C4	C3	120(2)
C1	C6	C7	117.1(18)	N2	C7	C6	118.4(17)
C5	C6	C7	125.0(17)	O3 ¹	C7	C6	119.8(18)
C14	C13	C12	116(2)	O3	C7	C6	119.8(18)
N3	C8	N2	115.4(19)	O3 ¹	C7	N2	121.8(18)
N3	C8	S1	123.7(17)	O3	C7	N2	121.8(18)
N2	C8	S1	120.9(18)	O3 ¹	C7	O3	0(2)
C12	C11	C10	118(2)	C11	C10	C9	122(2)
C13	C14	C9	124.3(19)	C11	C10	Br1	120.0(17)
C13	C14	Br3	115.9(17)	C9	C10	Br1	118.3(15)

Table 3. (Continued).

Atom	Atom	Atom	Angle (°)	Atom	Atom	Atom	Angle (°)
C9	C14	Br3	119.8(15)	C14	C9	C10	116.5(18)
C13	C12	Br2	120.0(16)	C14	C9	N3	119.6(17)
C11	C12	C13	122.7(19)	C10	C9	N3	123.6(17)
C11	C12	Br2	117.3(16)	O2	N1	C3	120(2)
C3	C2	C1	120(2)	O1	N1	C3	122(2)
C6	C1	C2	120(2)	O1	N1	O2	118.8(19)
C2	C3	C4	120.5(19)	C8	N3	C9	123.8(17)
C2	C3	N1	118.0(19)	C8	N2	C7	127.7(18)
C4	C3	N1	121(2)	O3 ¹	O3	C7	0(10)
C4	C5	C6	121(2)				

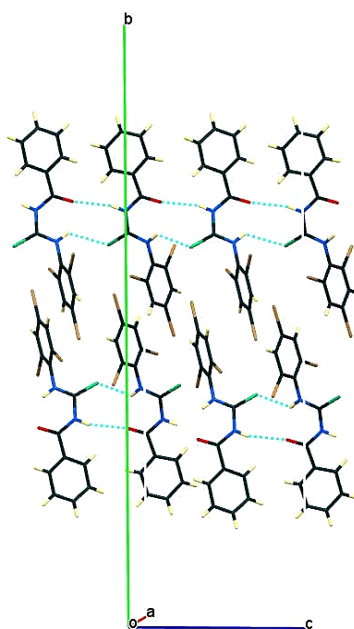
¹ Symmetry code: +x, +y, +z.**Table 4.** Hydrogen bonds for compound I and II.

Compound	D	H	A	d(D-H) (Å)	d(H-A) (Å)	d(D-A) (Å)	D-H-A (°)	Symmetry
I	C4	H4	Br5	0.93	2.91	3.827(13)	168.6	2-x, 1-y, 1-z
	C16	H16	Br2	0.93	3.02	3.937(16)	167.4	1-x, 1-y, 1-z
	N2	H22	O2	0.86	2.43	3.273(17)	165.9	+x, +y, -1+z
	N3	H33	S1	0.86	2.76	3.353(13)	127.2	+x, +y, 1+z
II	N3	H3	O3	0.86	1.88	2.57(2)	137.0	x, +y, +z
	N2	H2A	S1	0.86	2.77	3.616(17)	167.7	1-x, 2-y, 1-z

Table 5. Experimental, calculated, and tentative of some relevant vibrational modes (cm⁻¹) of compounds I and II.

Compound I		Compound II		Assignment *
Experimental	Calculated	Experimental	Calculated	
3255	3617	3413	3674	v(N1-H)
3112	3515	3284	3339	v(N2-H)
3099	3261	3180	3172	v(C-H) _{Ar}
3074	3198	3073	3081	v(C-H) _{Ar}
1670	1665	1728	1734	vC=O
1603	1605	1607	1606	vC=C
1506	1499	1539	1532	vN-CS
1343	1390	1381	1471	vN-CO
-	-	1346	1359	vN=O
1262	1258	1276	1270	vCS-N
861	875	858	890	vC=S
842	811	842	874	δC=S
778	793	729	796	vC-Br1
739	791	705	730	vC-Br2
701	742	700	686	vC-Br3

*v: Stretching, δ: Bending.

**Figure 3.** Molecular packing diagram of compound I.

Moreover, the vN-H vibration peaks were observed for the thiourea group at 3112 and 3284 cm⁻¹ for compounds I and II, respectively. Furthermore, the calculated values for the stretching vibrations were found to be 3617, 3515 and 3674, 3339 cm⁻¹, respectively. Although the stretching vibrations of the carbonyl (vC=O) and thiocarbonyl (vC=S) groups as an

experimental value were observed at 1670, 1728 cm⁻¹ and 1343, 1454 cm⁻¹, for compounds I and II, that of theoretical values was founded at 1665, 1734 cm⁻¹ and 1390, 1471 cm⁻¹, respectively. Furthermore, the presence of the bending vibration of the C = S group for the title compounds was identified by the observed peak at 861 and 858 cm⁻¹ [30].

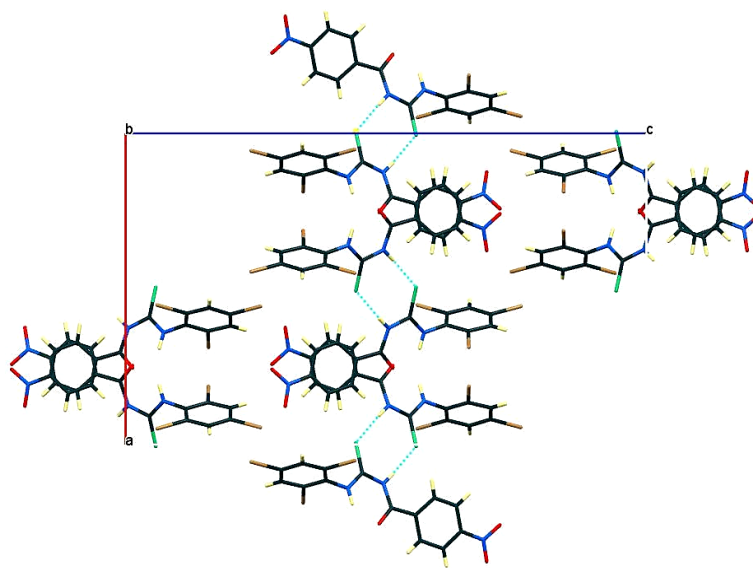


Figure 4. Molecular packing diagram of compound II.

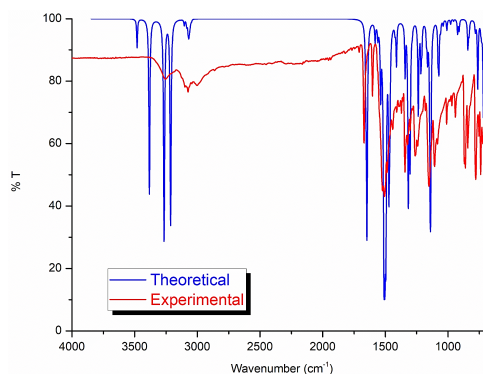


Figure 5. Experimental and simulated FT-IR spectra of compound I.

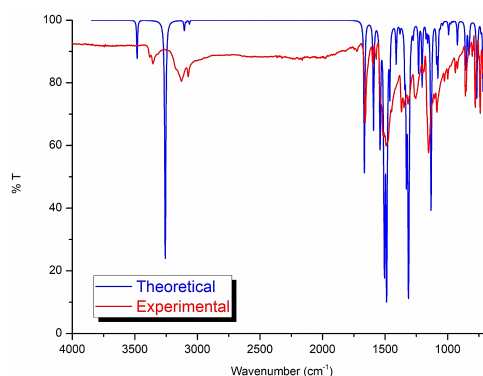
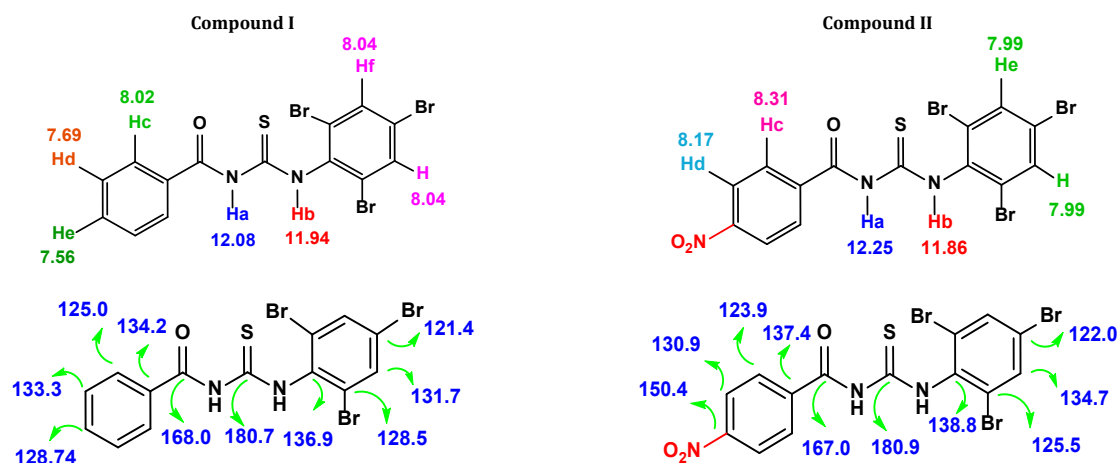


Figure 6. Experimental and simulated FT-IR spectra of compound II.

Vibration bands with wavenumbers of 3099, 3074 and 3180, 3073 cm^{-1} ($\nu\text{C-H, Ar-H}$); 1603 and 1607 cm^{-1} ($\nu\text{C=C}$); 1506 and 1539 cm^{-1} ($\nu\text{N-CS}_{\text{thioureido}}$), 1262 and 1276 cm^{-1} ($\nu\text{CS-N}$) were confirmed the title compounds I and II, respectively. The O-NO stretching vibration was observed at 1346 cm^{-1} for the title compound II [31]. The stretching of the C-Br bonds in the compounds was confirmed at 778, 739, 701 cm^{-1} and 729, 705, and 700 cm^{-1} , respectively. These stretching bands of the C-Br bonds were also calculated as 791, 793, 742 cm^{-1} , and 796, 730, 686 cm^{-1} for compounds I and II, respectively. All conclusions agree with the literature [32,33].

3.2.2. NMR analysis

In most compounds containing electronegative atoms, N-H values are observed around δ 12 ppm due to hydrogen bond formation [34]. In ^1H NMR, the characteristic broad singlet peaks appeared at δ 12.08, 12.25 ppm and 11.94, 11.86 ppm, for amide protons (NH_a) and thio-amide protons (NH_b) confirmed the structure of the new compounds I and II, respectively [35-37]. For the title compounds I and II, the aromatic proton peaks of the phenyl ring and the 4-nitrophenyl ring could be observed at δ 7.56 ppm (t, 1H, $-\text{H}_a$), 7.69 (t, 2H, $-\text{H}_e$), 8.02 (d, 2H, $-\text{H}_c$) and



Scheme 2. The ^1H NMR and ^{13}C NMR chemical shifts of the title compounds I and II in $\text{DMSO}-d_6$.

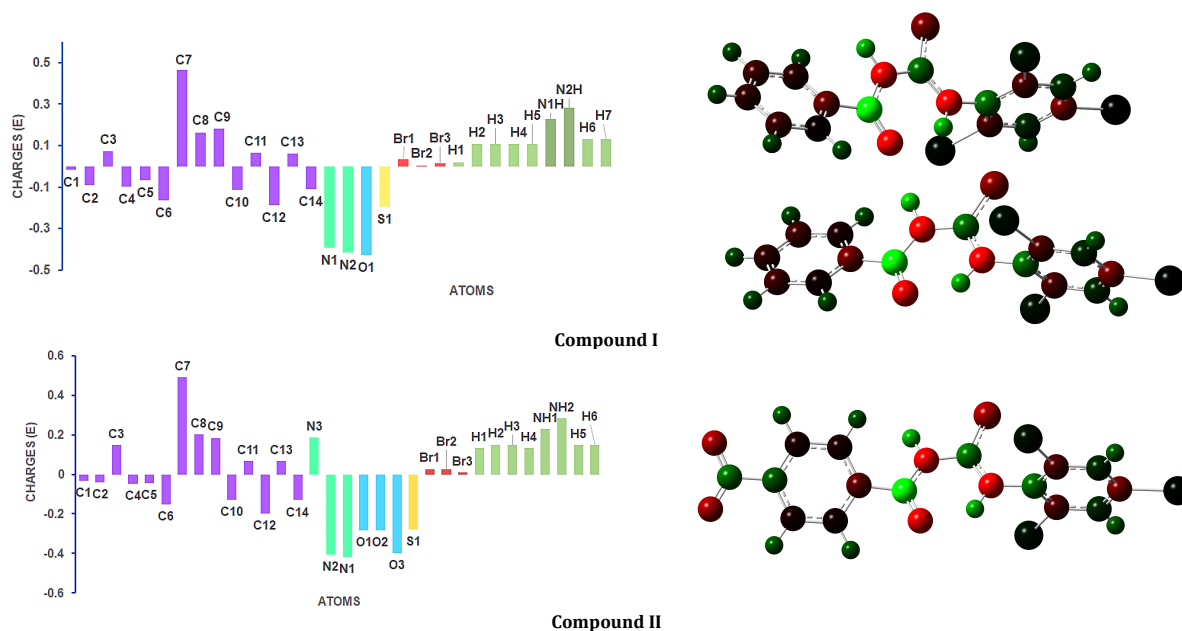


Figure 7. The Mulliken atomic charge distribution of compounds I and II in the gas phase.

8.17 (d, 2H, -Ha), 8.31 ppm (d, 2H, -Hc), respectively. Furthermore, two similar proton peaks of the 2,4,6-tribromo-phenyl ring of compounds I and II were observed at δ 8.04 (s, 2H, H_f) and 7.99 ppm (s, 2H, H_e), respectively. In the ^{13}C NMR spectra of title compounds I and II, the signals observed in the region of δ 168.0 and 167.0 ppm and δ 180.7 and δ 180.9 ppm clearly describe the C=O and C=S carbons, respectively. Additionally, the peaks observed in the aromatic region confirmed the structures (Scheme 2).

3.3. Mulliken atomic charge analysis

Because atomic charges determine the dipole moment, the molecular polarization and bond properties of a molecule. The calculation of the Mulliken atomic charge plays an important role [38]. The Mulliken population analysis was performed using the DFT/B3LYP calculation method with 6-311+G(d,p) basis set for the title compounds. Graphical reorientations of the Mulliken charge distribution of the title compounds I and II are shown in Figure 7. The hydrogen atoms are all positively charged, but those bonded to the nitrogen atoms are the most positively charged. Similarly, the nitrogen atoms conjugated

with the carbonyl and thiocarbonyl groups of the title compounds I and II are highly negative charges (-0.392, -0.414 esu and -0.407, -0.418 esu), respectively, while the nitrogen atom of the nitro group of compound II has a positive charge (0.186 esu). In compounds I and II, it has been observed that the carbon atoms in the phenyl ring to which it is attached have a negative charge, while the bromine atoms have very little positive charge 0.004-0.017 esu and 0.009-0.027 esu, respectively. The highest positive atomic charge was 0.466 in compound I, but also with 0.492 compound II has a higher positive carbon atom charge of the carbonyl group. Therefore, carbonyl groups are a reactive moiety in these compounds.

3.4. Molecular electrostatic potential (MEP)

The molecular electrostatic potential (MEP) helps interpret detailed information about many properties of a compound, such as chemical reactivity or biological activity. The spatial distribution and values of the electrostatic potential determine the attack regions of an electrophilic or nucleophilic unit on the molecule [39].

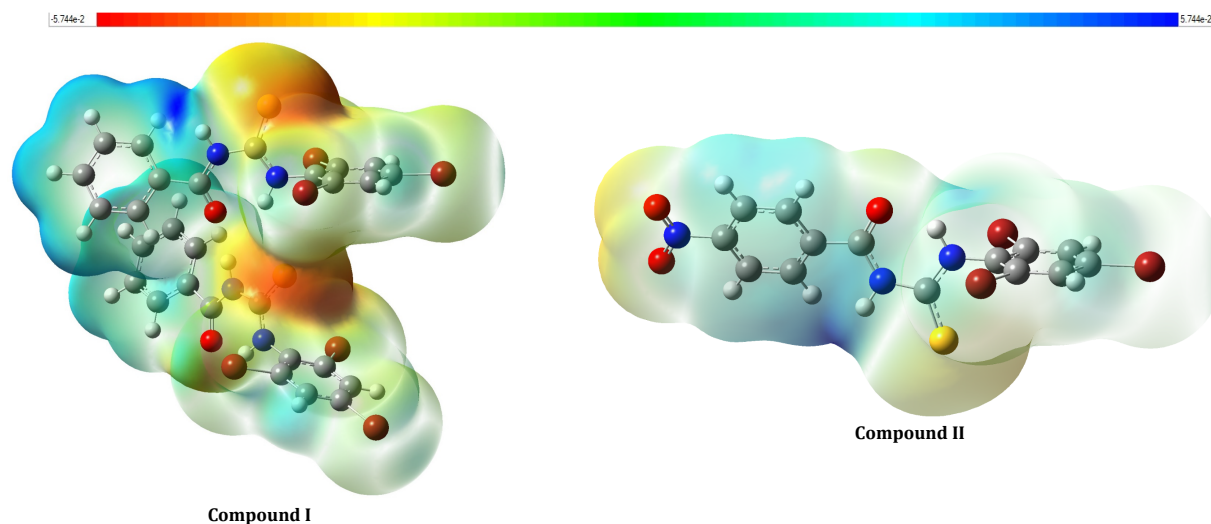


Figure 8. Molecular electrostatic potential (MEP) maps calculated of the title compounds I and II at B3LYP/6-311G(d,p) level.

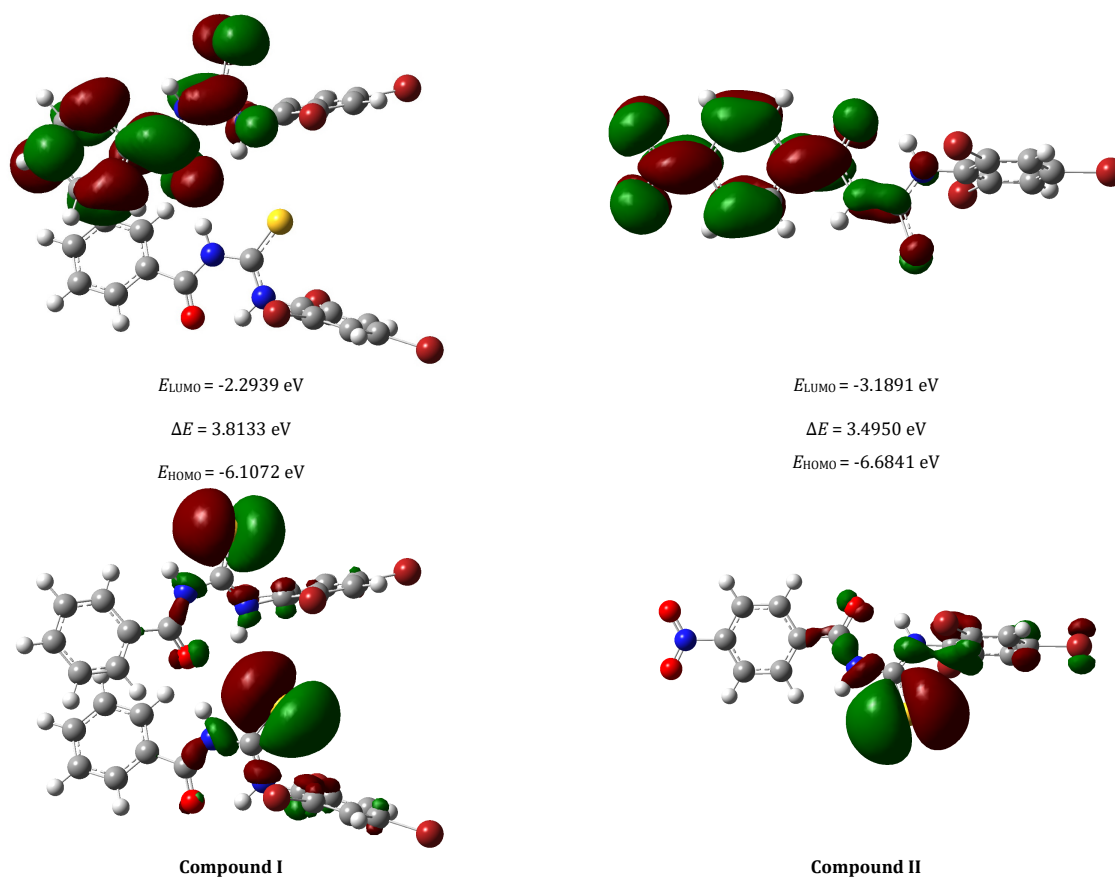


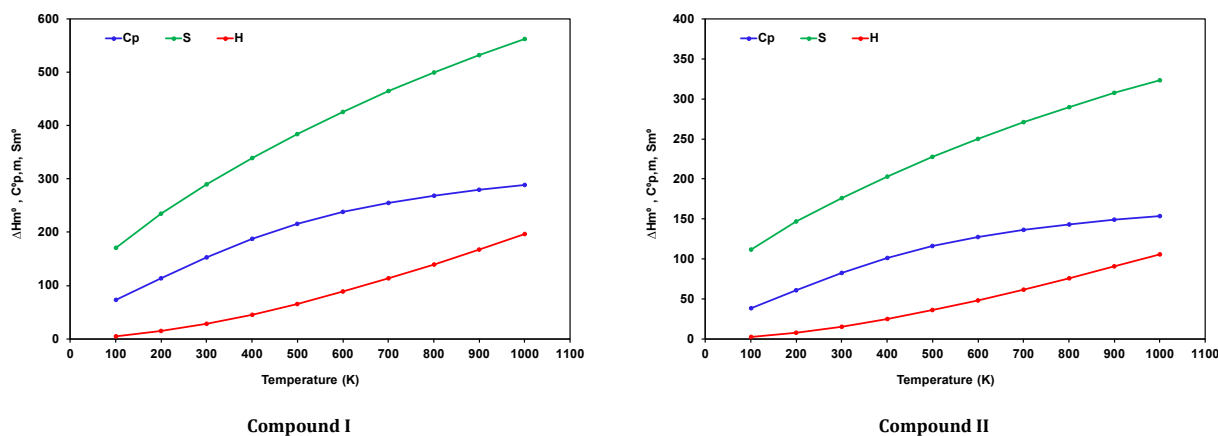
Figure 9. HOMO-LUMO plot of compounds I and II.

The total electronic density and the MEP surface of the title molecules are constructed using the B3LYP/6-311G (d,p) method and are shown in Figure 8. Electronegative and electropositive regions of the MEP surface are identified by the color scheme. The red color is rich in electrons and partially negatively charged; yellow and green are defined as neutral ranges and blue is defined as the electron-deficient, partially positive charge region [40]. These MEP maps for compounds I and II show that the sulfur atom, as well as the carbonyl oxygen atom, is a possible site for electrophilic attack due to the

tribromophenyl ring, and the nucleophilic attack sites are located on the hydrogen atoms bonded to nitrogen atoms. These MEP maps for compounds I and II show that the S atom, as well as the carbonyl O atom, is a possible site for electrophilic attack due to the tribromophenyl ring, and the nucleophilic attack sites are located on the hydrogen atoms bonded to nitrogen atoms. The results show that the most reactive region of these compounds is the region containing the sulfur atom, and provide information about the region where the compound may have intermolecular hydrogen bond interactions.

Table 6. Frontier orbital energy, HOMO-LUMO energy gap, ionization potential (I), electron affinity (A), chemical potential (μ), chemical hardness (η), absolute softness (ζ), absolute electronegativity (χ), chemical potential (μ), and electrophilicity index (ω) of title compounds for ground state geometries in gas phase at B3LYP/6-311G(d,p) level.

Parameters B3LYP/6-311G(d,p)	Compound I	Compound II
Electronic energy (a.u.)	-17688.9911	-9049.0604
E_{HOMO} (eV)	-6.1072	-6.6841
E_{LUMO} (eV)	-2.2939	-3.1891
Ionization energy, $I = -E_{\text{HOMO}}$ (eV)	6.1072	6.6841
Electron affinity, $A = -E_{\text{LUMO}}$ (eV)	2.2939	3.1891
Energy band gap, $\Delta E = E_{\text{HOMO}} - E_{\text{LUMO}}$ (eV)	3.8133	3.4950
Chemical hardness, $\eta = (I-A)/2$ (eV)	1.9066	1.7475
Chemical softness, $\zeta = 1/2\eta$ (eV ⁻¹)	0.2622	0.2861
Electronegativity, $\chi = (I+A)/2$ (eV)	4.2005	4.9366
Chemical potential, $\mu = -(I+A)/2$ (eV)	-4.2005	-4.9366
Electrophilicity index, $\omega = \mu^2/2\eta$ (eV)	4.6271	6.9728

**Figure 10.** Thermodynamic parameters of compounds I and II.

3.5. Frontier molecular orbitals analysis

Frontier molecular orbitals (FOMs), known as the highest occupied molecular orbital (HOMO) and the lowest unoccupied molecular orbital (LUMO), contain information on the chemical stability of the molecule [41]. Active regions can be predicted by the distribution of the frontier orbital since the HOMO implies the electron-donating capacity of a molecule and the LUMO indicates the electron-accepting capacity of a molecule [42]. The HOMO-LUMO plots of the two molecules are shown in Figure 9. The negative and positive phases are colored red and green. As shown in Figure 9, the HOMO electrons are localized around the entire tribromophenyl and connected thiourea moiety, while for LUMO, the electrons are distributed entirely over the aroyl ring and the thiourea moiety for the title compounds.

The electron-withdrawing or donating groups influence the HOMO and LUMO energies. Electron-withdrawing groups, such as nitro groups, reduce the energy of the LUMO while affecting the HOMO slightly less. It has been described that a molecule with a small frontier orbital space can be more polarizable and is generally associated with high chemical reactivity and low kinetic stability, and is called a soft molecule [43]. Global reactivity, such as Frontier orbital energy, HOMO-LUMO energy gap, chemical potential (μ), chemical hardness (η), global electrophilicity index (ω), and chemical softness (ζ) were calculated using the B3LYP/6-311G(d,p) method and is listed in Table 6. The energy values of the HOMO and LUMO of the title compounds (I, II) were calculated as -6.1072 eV (HOMO), -6.2569 eV (HOMO-1), -2.2939 eV (LUMO), -2.0563 eV (LUMO-1) and -6.6841 eV (HOMO), -6.9641 eV (HOMO-1), -3.1891 eV (LUMO), -1.9157 eV (LUMO+1), respectively (Table 6). According to these data, the energy gap values for compounds I and II are calculated as 3.8133 eV and 3.4950 eV. When comparing the energy gap values of the title compounds, compound II is more chemically reactive and unstable than

compound I because the energy gap is narrower due to the effect of the nitro group [44-45]. From Table 6, when the chemical hardness and softness values of compounds I and II (1.7475 eV, 0.2861 eV and 1.9066 eV, 0.2622 eV, respectively) are compared, it is emphasized that compound II is more reactive than compound I [46].

3.6. Thermodynamic properties

Thermodynamic quantum chemical data becomes important to study the reaction processes of organic compounds [47]. Thermodynamic parameters for different temperatures were calculated at the B3LYP/6-311G (d,p) level and scaled by 0.96. Three main thermodynamic properties as heat capacity $C_{p,m}^\circ$, enthalpy ΔH_m° and entropy S_m° for compounds I and II are plotted in Figures 10a and 10b. As shown in Figure 10, all values increase as the temperature increases in the range of 100-1000 K.

The correlation equation of $C_{p,m}^\circ$, S_m° , ΔH_m° and temperature are as follows for title compounds I and II, respectively:

$$C_{p,m}^\circ (\text{I}) = 26.5639 + 0.4899 T - 2.3069 \times 10^{-4} T^2 \quad (R^2 = 0.9992) \quad (1)$$

$$S_m^\circ (\text{I}) = 112.2255 + 0.6415 T - 1.93958 \times 10^{-4} T^2 \quad (R^2 = 0.9996) \quad (2)$$

$$\Delta H_m^\circ (\text{I}) = -7.5617 + 0.0884 T + 7.4451 \times 10^{-6} T^2 \quad (R^2 = 0.9993) \quad (3)$$

$$C_{p,m}^\circ (\text{II}) = 13.7884 + 0.2660 T - 1.279 \times 10^{-4} T^2 \quad (R^2 = 0.9991) \quad (4)$$

$$S_m^\circ (\text{II}) = 79.7534 + 0.3501 T - 1.0782 \times 10^{-4} T^2 \quad (R^2 = 0.9996) \quad (5)$$

$$\Delta H_m^\circ (\text{II}) = -4.2287 + 0.0491 T + 6.1967 \times 10^{-5} T^2 \quad (R^2 = 0.9993) \quad (6)$$

Additionally, for both title compounds, all calculated thermodynamic parameters ($C_{p,m}^\circ$, S_m° , ΔH_m°) appear to increase

with increasing temperature due to the increase in molecular vibration.

4. Conclusions

In this study, two novel *N*-benzoyl-*N'*-tribromophenyl thiourea (I) and 4-nitrobenzoyl-*N'*-tribromophenylthiourea (II) have been synthesized and investigated by elemental analysis, FT-IR, ¹H NMR, ¹³C NMR, and X-ray diffraction techniques. The crystal structures of compounds I and II showed intramolecular and intermolecular interactions with centers that are hydrogen-bond donors and hydrogen-bond acceptors. The presence of electron donors such as S, N, and O in these compounds emphasizes their polydentate ligand properties. This property would cause compounds I and II to exhibit polydentate ligand properties with respect to various metals in terms of coordination chemistry. Theoretical calculations of these compounds have also been performed using the density functional theory method with the B3LYP/6-311G(d,p) basis set. Although the differences in the geometric parameters are observed, the general agreement is in a good range and the theoretical calculations support the solid-state structures. The experimental vibrational frequencies agree with the results of the B3LYP method. The calculated MEP maps verify the intramolecular hydrogen-bond interactions in the solid state. HOMO and LUMO's come into existence with π -antibonding type orbitals. It is clear from the global reactivity data that compound I (X = H) is hard and more stable or less reactive, while compound II (X = NO₂) is soft and less stable.

Acknowledgements

The authors are grateful to Prof. Kadir Arslan at Morgan State University, Baltimore, USA, for his financial support.

Supporting information

CCDC-2160417 (Compound I) and 2160418 (Compound II) contain the supplementary crystallographic data for this paper. These data can be obtained free of charge via www.ccdc.cam.ac.uk/data_request/cif, or by e-mailing data_request@ccdc.cam.ac.uk, or by contacting The Cambridge Crystallographic Data Centre, 12 Union Road, Cambridge CB2 1EZ, UK; fax: +44(0)1223-336033.

Disclosure statement

Conflict of interest: The authors declare that they have no conflict of interest. Ethical approval: All ethical guidelines have been adhered to. Sample availability: Samples of the compounds are available from the author.

CRedit authorship contribution statement

Conceptualization: Fatma Aydin; Methodology: Fatma Aydin; Software: Nahide Burcu Arslan; Formal Analysis: Nahide Burcu Arslan; Investigation: Fatma Aydin; Data Curation: Fatma Aydin, Nahide Burcu Arslan; Writing - Original Draft: Fatma Aydin; Writing - Review and Editing: Fatma Aydin, Nahide Burcu Arslan; Visualization: Fatma Aydin, Nahide Burcu Arslan; Supervision: Fatma Aydin; Project Administration: Fatma Aydin.

ORCID and Email

Nahide Burcu Arslan

 burcu.arslan@giresun.edu.tr

 <https://orcid.org/0000-0002-1880-1047>

Fatma Aydin

 faydin@comu.edu.tr

 <https://orcid.org/0000-0002-7219-6407>

References

[1]. Özgeriş, B. Design, synthesis, characterization, and biological evaluation of nicotinoyl thioureas as antimicrobial and antioxidant agents. *J. Antibiot. (Tokyo)* **2021**, *74*, 233–243.

- [2]. Rana, A.; Siddiqui, N.; Khan, S. A.; Ehtaishamul Haque, S.; Bhat, M. A. N-[(6-Substituted-1,3-benzothiazole-2-yl)amino]carbonothioyl-2/[4-substituted benzamides: Synthesis and pharmacological evaluation. *Eur. J. Med. Chem.* **2008**, *43*, 1114–1122.
- [3]. Asghar, F.; Rana, S.; Fatima, S.; Badshah, A.; Lal, B.; Butler, I. S. Biologically active *halo*-substituted ferrocenyl thioureas: synthesis, spectroscopic characterization, and DFT calculations. *New J Chem* **2018**, *42*, 7154–7165.
- [4]. Soni, L. K.; Narsinghani, T.; Jain, R. Synthesis and antibacterial screening of some 1-aroyl-3-aryl thiourea derivatives. *ISRN Med. Chem.* **2014**, *2014*, 1–6, 393102.
- [5]. Duan, L.-P.; Xue, J.; Xu, L.-L.; Zhang, H.-B. Synthesis 1-Acyl-3-(2'-aminophenyl) thioureas as Anti-Intestinal Nematode Prodrugs. *Molecules* **2010**, *15*, 6941–6947.
- [6]. Shaabanzadeh, M.; Khabari, F. One-pot diastereoselective synthesis of new spiro indenquinoxaline derivatives containing cyclopropane ring. *ARKIVOC* **2009**, *2009*, 307–315.
- [7]. Aydin, F.; Ünver, H.; Aykaç, D.; İskeleli, N. O. Spectroscopic studies and structure of 4-(3-benzoylthioureido)benzoic acid. *J. Chem. Crystallogr.* **2010**, *40*, 1082–1086.
- [8]. Ozer, C. K.; Binzet, G.; Arslan, H. Crystal and molecular structure of bis(N-(diethylcarbamothioyl)cyclohexane carboxamido)copper(II) complex. *Eur. J. Chem.* **2020**, *11*, 319–323.
- [9]. Solmaz, U.; Gumus, I.; Binzet, G.; Celik, O.; Balci, G. K.; Dogen, A.; Arslan, H. Synthesis, characterization, crystal structure, and antimicrobial studies of novel thiourea derivative ligands and their platinum complexes. *J. Coord. Chem.* **2018**, *71*, 200–218.
- [10]. Luckay, R. C.; Mebrahtu, F.; Esterhuysen, C.; Koch, K. R. Extraction and transport of gold(III) using some acyl(aro)ylthiourea ligands and a crystal structure of one of the complexes. *Inorg. Chem. Commun.* **2010**, *13*, 468–470.
- [11]. Aydin, F.; Aykaç, D.; Burcu Arslan, N.; Kazak, C. Synthesis, characterization, and crystal structure of bis[4-(3'-benzoyl)thiocarbamidophenyl]ether. *Crystallogr. Rep.* **2014**, *59*, 955–960.
- [12]. Contreras Aguilar, E.; Echeverría, G. A.; Piro, O. E.; Ulic, S. E.; Jios, J. L.; Tuttolomondo, M. E.; Molina, R. D. I.; Arena, M. E. Acyl thiourea derivatives: A study of crystallographic, bonding, biological and spectral properties. *Chem. Phys. Lett.* **2019**, *715*, 64–71.
- [13]. Aydin, F.; Arslan, N. B. Synthesis, crystal structure and cyclic voltammetric behavior of N-aroyl-N'-(4'-cyanophenyl)thioureas. *Molbank* **2022**, *2022*, M1316.
- [14]. Pinter, B.; Fievez, T.; Bickelhaupt, F. M.; Geerlings, P.; De Proft, F. On the origin of the steric effect. *Phys. Chem. Chem. Phys.* **2012**, *14*, 9846.
- [15]. Geiger, T.; Haupt, A.; Maichle-Mössner, C.; Schrenk, C.; Schnepf, A.; Bettinger, H. F. Synthesis and photodimerization of 2- and 2,3-disubstituted anthracenes: Influence of steric interactions and London dispersion on diastereoselectivity. *J. Org. Chem.* **2019**, *84*, 10120–10135.
- [16]. Audu, O. Y.; Jooste, J.; Malan, F. P.; Ajani, O. O.; October, N. Synthesis, characterization, molecular structure, and computational studies on 4(1H)-pyran-4-one and its derivatives. *J. Mol. Struct.* **2021**, *1245*, 131077.
- [17]. Udofia, I. A.; Trust Ekama; Ogunbayo, T. B.; Oloba-Whenu, O. A.; Rhyman, L.; Isanbor, C.; Ramasami, P. Experimental and theoretical calculation of pKa values of substituted-2,4,6-trinitrodiphenylamines. *J. Mol. Liq.* **2023**, *371*, 120926.
- [18]. Sheldrick, G. M. SHELXS-97 and SHELXL-97 Program for Crystal Structure Solution and Refinement. University of Gottingen, Germany, 1997.
- [19]. Farrugia, L. J. WinGX and ORTEP for Windows: an update. *J. Appl. Crystallogr.* **2012**, *45*, 849–854.
- [20]. Becke, A. D. Density-functional thermochemistry. III. The role of exact exchange. *J. Chem. Phys.* **1993**, *98*, 5648–5652.
- [21]. Lee, C.; Yang, W.; Parr, R. G. Development of the Colle-Salvetti correlation-energy formula into a functional of the electron density. *Phys. Rev. B Condens. Matter* **1988**, *37*, 785–789.
- [22]. Ditchfield, R.; Hehre, W. J.; Pople, J. A. Self-consistent molecular-orbital methods. IX. An extended Gaussian-type basis for molecular-orbital studies of organic molecules. *J. Chem. Phys.* **1971**, *54*, 724–728.
- [23]. Frisch, M. J.; Trucks, G. W.; Schlegel, H. B.; Scuseria, G. E.; Robb, M. A.; Cheeseman, J. R.; Montgomery, J. A.; Vreven, T.; Kudin, K. N.; Burant, J. C.; Millam, J. M.; Iyengar, S. S.; Tomasi, J.; Barone, V.; Mennucci, B.; Cossi, M.; Scalmani, G.; Rega, N.; Petersson, G. A.; Nakatsuji, H.; Hada, M.; Ehara, M.; Toyota, K.; Fukuda, R.; Hasegawa, J.; Ishida, M.; Nakajima, T.; Honda, Y.; Kitao, O.; Nakai, H.; Klene, M.; Li, X.; Knox, J. E.; Hratchian, H. P.; Cross, J. B.; Adamo, C.; Jaramillo, J.; Gomperts, R.; Stratmann, R. E.; Yazyev, O.; Austin, A. J.; Cammi, R.; Pomelli, C.; Ochterski, J. W.; Ayala, P. Y.; Morokuma, K.; Voth, G. A.; Salvador, P.; Dannenberg, J. J.; Zakrzewski, V. G.; Dapprich, S.; Daniels, A. D.; Strain, M. C.; Farkas, O.; Malick, D. K.; Rabuck, A. D.; Raghavachari, K.; Foresman, J. B.; Ortiz, J. V.; Cui, Q.; Baboul, A. G.; Clifford, S.; Cioslowski, J.; Stefanov, B. B.; Liu, G.; Liashenko, A.; Piskorz, P.; Komaromi, I.; Martin, R. L.; Fox, D. J.; Keith, T.; Al-Laham, M. A.; Peng, C. Y.; Nanayakkara, A.; Challacombe, M.; Gill, P. M. W.; Johnson, B.; Chen, W.;

- Wong, M. W.; Gonzalez, C.; Pople, J. A. Gaussian09, Gaussian, Inc., Wallingford CT, 2009.
- [24]. *Molecular electrostatic potentials: Volume 3: Concepts and applications*; Murray, J. S.; Sen, K., Eds.; Elsevier Science: London, England, ISBN: 978-0-444-82353-3, 1996.
- [25]. Andersson, M. P.; Uvdal, P. New scale factors for harmonic vibrational frequencies using the B3LYP density functional method with the triple- ζ basis set 6-311+G(d,p). *J. Phys. Chem. A* **2005**, *109*, 2937–2941.
- [26]. Dennington, R.; Keith, T. A.; Millam, J. M. GaussView, Version 5, Semichem Inc.; Shawnee Mission, KS, 2009.
- [27]. Threlfall, T. The infrared spectra of amides. Part 1. The stretching vibrations of primary carboxamides. *Vib. Spectrosc.* **2022**, *121*, 103386.
- [28]. Larkin, P. *Infrared and Raman spectroscopy: Principles and spectral interpretation*; Elsevier Science Publishing: Philadelphia, PA, 2018.
- [29]. Hassan, I. N. Synthesis, spectral characterization and crystal structural of 1-(2-Morpholinoethyl)-3-(3-phenylacryloyl)thiourea. *Int. J. Phys. Sci.* **2011**, *6*.
- [30]. Estévez-Hernández, O.; Otazo-Sánchez, E.; Hidalgo-Hidalgo de Cisneros, J. L.; Naranjo-Rodríguez, I.; Reguera, E. A Raman and infrared study of 1-furoyl-3-monosubstituted and 3,3-disubstituted thioureas. *Spectrochim. Acta A Mol. Biomol. Spectrosc.* **2005**, *62*, 964–971.
- [31]. Kirishnamaline, G.; Magdaline, J. D.; Chithambarathane, T.; Aruldas, D.; Anuf, A. R. Theoretical investigation of structure, anticancer activity and molecular docking of thiourea derivatives. *J. Mol. Struct.* **2021**, *1225*, 129118.
- [32]. Asghar, F.; Fatima, S.; Rana, S.; Badshah, A.; Butler, I. S.; Tahir, M. N. Synthesis, spectroscopic investigation, and DFT study of *N,N'*-disubstituted ferrocene-based thiourea complexes as potent anticancer agents. *Dalton Trans.* **2018**, *47*, 1868–1878.
- [33]. Khurshid, A.; Saeed, A.; Shabir, G.; Gil, D. M.; Bolte, M.; Erben, M. F. Synthesis of phenazone based carboxamide under thiourea reaction conditions. Molecular and crystal structure, Hirshfeld surface analysis and intermolecular interaction energies. *J. Mol. Struct.* **2023**, *1278*, 134948.
- [34]. Hansen, P. E.; Vakili, M.; Kamounah, F. S.; Spanget-Larsen, J. NH stretching frequencies of intramolecularly hydrogen-bonded systems: An experimental and theoretical study. *Molecules* **2021**, *26*, 7651.
- [35]. Qiao, L.; Zhang, Y.; Hu, W.; Guo, J.; Cao, W.; Ding, Z.; Guo, Z.; Fan, A.; Song, J.; Huang, J. Synthesis, structural characterization and quantum chemical calculations on 1-(isomeric methylbenzoyl)-3-(4-trifluoromethylphenyl)thioureas. *J. Mol. Struct.* **2017**, *1141*, 309–321.
- [36]. Saeed, A.; Khurshid, A.; Bolte, M.; Fantoni, A. C.; Erben, M. F. Intra- and intermolecular hydrogen bonding and conformation in 1-acyl thioureas: An experimental and theoretical approach on 1-(2-chlorobenzoyl)thiourea. *Spectrochim. Acta A Mol. Biomol. Spectrosc.* **2015**, *143*, 59–66.
- [37]. Özer, C. K.; Arslan, H.; VanDerveer, D.; Külcü, N. Synthesis and characterization of N-(arylcabamothioyl)-cyclohexanecarboxamide derivatives: The crystal structure of N-(naphthalen-1-ylcabamothioyl)cyclohexanecarboxamide. *Molecules* **2009**, *14*, 655–666.
- [38]. Mulliken, R. S. Electronic population analysis on LCAO–MO molecular wave functions. I. *J. Chem. Phys.* **1955**, *23*, 1833–1840.
- [39]. Scrocco, E.; Tomasi, J. Electronic molecular structure, reactivity and intermolecular forces: An heuristic interpretation by means of electrostatic molecular potentials. In *Advances in Quantum Chemistry Volume 11*; Elsevier, 1978; pp. 115–193.
- [40]. Toro-Labbé, A. *Theoretical aspects of chemical reactivity*; Elsevier Science: London, England, 2007.
- [41]. Pearson, R. G. Chemical hardness and density functional theory. *J. Chem. Sci. (Bangalore)* **2005**, *117*, 369–377.
- [42]. Xu, Y.; Chu, Q.; Chen, D.; Fuentes, A. HOMO–LUMO gaps and molecular structures of polycyclic aromatic hydrocarbons in soot formation. *Front. Mech. Eng.* **2021**, *7*.
- [43]. Fleming, I. *Molecular orbitals and organic chemical reactions*; Wiley, New York, 2010.
- [44]. Türker, L. Interaction of TNT and aluminum – A DFT treatment. *Z. Anorg. Allg. Chem.* **2015**, *641*, 408–413.
- [45]. Gökalp, F. A theoretical investigation of TNT in different phases by using DFT. *Turkish Computational and Theoretical Chemistry* **2019**, *3*, 1–4.
- [46]. Miar, M.; Shiroudi, A.; Pourshamsian, K.; Oliaey, A. R.; Hatamjafari, F. Theoretical investigations on the HOMO–LUMO gap and global reactivity descriptor studies, natural bond orbital, and nucleus-independent chemical shifts analyses of 3-phenylbenzo[d]thiazole-2(3H)-imine and its *para*-substituted derivatives: Solvent and substituent effects. *J. Chem. Res.* **2021**, *45*, 147–158.
- [47]. Jean-Pierre, L. The role and the status of thermodynamics in quantum chemistry calculations. In *Thermodynamics - Interaction Studies - Solids, Liquids and Gases*; InTech, ISBN: 978-953-307-563-1, 2011.



Copyright © 2024 by Authors. This work is published and licensed by Atlanta Publishing House LLC, Atlanta, GA, USA. The full terms of this license are available at <https://www.eurjchem.com/index.php/eurjchem/terms> and incorporate the Creative Commons Attribution-Non Commercial (CC BY NC) (International, v4.0) License (<http://creativecommons.org/licenses/by-nc/4.0>). By accessing the work, you hereby accept the Terms. This is an open access article distributed under the terms and conditions of the CC BY NC License, which permits unrestricted non-commercial use, distribution, and reproduction in any medium, provided the original work is properly cited without any further permission from Atlanta Publishing House LLC (European Journal of Chemistry). No use, distribution, or reproduction is permitted which does not comply with these terms. Permissions for commercial use of this work beyond the scope of the License (<https://www.eurjchem.com/index.php/eurjchem/terms>) are administered by Atlanta Publishing House LLC (European Journal of Chemistry).